

Cs₃AgAs₄Se₈ and CsAgAs₂Se₄: Selenoarsenates with Infinite ¹_∞[AsSe₂][−] Chains in Different Ag⁺ Coordination Environments

M. Wachhold and M. G. Kanatzidis*

Department of Chemistry and Center for Fundamental Materials Research, Michigan State University, East Lansing, Michigan 48824

Received January 5, 2000

Two quaternary silver selenoarsenates Cs₃AgAs₄Se₈ (**I**) and CsAgAs₂Se₄ (**II**) have been discovered by methanothermal reaction of Li₃AsSe₃ with AgBF₄ in the presence of the respective alkali metal sources Cs₂CO₃ and CsCl. Orange crystals of Cs₃AgAs₄Se₈ (**I**) were formed after reaction at 120 °C for 72 h, whereas red CsAgAs₂Se₄ (**II**) was obtained under slightly different conditions at 140 °C for 70 h. Both compounds possess novel two-dimensional (2D) polyanions consisting of infinite ¹_∞[AsSe₂][−] chains that are interconnected by Ag⁺ ions in different coordination patterns. In **I**, a double layer of ¹_∞[AsSe₂][−] chains is bridged by distorted trigonal planar coordinated Ag⁺ atoms to form a ²_∞[AgAs₄Se₈]^{3−} layer with a thickness of about 11.3 Å. The nonbonding Ag··Ag distances are about 4.220 Å, and large cavities within the layers accommodate for three of the four crystallographic Cs⁺ cations. The double amount of Ag⁺ atoms per AsSe₂ chain unit in **II** leads to simple layers ²_∞[AgAs₂Se₄][−] {=[Ag₂As₄Se₈]^{2−}} in which the Ag⁺ atoms are arranged in rows between the ¹_∞[AsSe₂][−] chains, with alternating Ag··Ag distances of 3.053(3) and 3.488(3) Å. Hereby the ¹_∞[AsSe₂][−] polyanions show a disorder within the *central* (−As−Se_b)− chain (b = bridging), while the positions of the terminal Se atoms (Se_t) remain unaffected. The thermal, optical, and spectroscopic properties of the compounds are reported. Both **I** and **II** melt with decomposition and are wide band gap semiconductors with values of 2.07 and 1.79 eV, respectively. Raman spectroscopic data show typical band patterns expected for infinite [AsSe₂][−] chains. *Crystal Data*: Cs₃AgAs₄Se₈ (**I**), monoclinic, C2/c, *a* = 25.212(2) Å, *b* = 8.0748(7) Å, *c* = 22.803(2) Å, β = 116.272(2)°, *Z* = 8; CsAgAs₂Se₄ (**II**), monoclinic, P2₁/n, *a* = 10.9211(1) Å, *b* = 6.5188(2) Å, *c* = 13.7553(3) Å, β = 108.956(1)°, *Z* = 4.

Introduction

In the past decade, solventothermal and molten flux methods^{1,2} have been successfully applied for the discovery of new chalcogenido compounds. Recently, we have shown that systematic investigations of a given reaction system can lead to hitherto unknown phases. For example, in the chalcoarsenate system, the strong condensation ability of the [AsQ₃]^{3−} unit (Q = S, Se) is well documented in a number of papers³ and has recently been summarized.⁴ These condensation reactions should depend on various reaction parameters, such as reaction time, temperature, or initial pH value, and their exploration should be useful in the context of exploratory synthesis. Using this approach for the heavier alkali metals K and Rb, we were able to synthesize four new Ag selenoarsenates, namely, K₃AgAs₂Se₅·0.25MeOH,⁴ K₂AgAs₃Se₆,⁴ Rb₂AgAs₃Se₆,⁴ and RbAg₂As₃Se₆.⁵

Prior to our investigations, only K₅Ag₂As₃Se₉ {=K₅−[Ag₂(AsSe₄)(As₂Se₅)]} was reported.⁶ A closer inspection of the employed reaction conditions for the synthesis of this set of compounds clearly shows that the reaction times can be closely correlated to the selenoarsenate building units in the observed structures. Short reaction times (e.g., hours) lead to K₃AgAs₂Se₅·0.25MeOH⁴ and RbAg₂As₃Se₆,⁵ their anions reveal isolated [As₂Se₅]^{4−} bitetrahedra and [As₃Se₆]^{3−} rings, a condensation product of two or three [AsSe₃]^{3−} units, respectively, followed by a ring closure reaction in the latter case. Extended reaction times (e.g., days) on the other hand lead to infinite chains ¹_∞[AsSe₂][−] in the isostructural A₂AgAs₃Se₆ compounds with A = K, Rb.⁴ K₅Ag₂As₃Se₉ could be obtained by the methanolothermal reaction at 110 °C for 1 week, and two selenoarsenate units with *three* different As oxidation states, namely, tetrahedral [As^VSe₄]^{3−} and the [Se₂As^{II}−As^{IV}Se₃]^{4−} anion with a direct As−As bond.⁶ This clearly demonstrates that complicated redox processes may also take place, given enough reaction time.

These interesting results led us to the conclusion that it would be worthwhile to study also the corresponding Cs⁺ system in the same manner, i.e., with changes in the various reaction parameters, since no compounds have been reported so far. As an outcome, we now report the synthesis, structural characterization, and properties of two new silver selenoarsenates Cs₃AgAs₄Se₈ (**I**) and CsAgAs₂Se₄ (**II**). Both compounds are structurally similar because they both possess sheet anions

- (1) (a) Sheldrick, W. S.; Wachhold, M. *Coord. Chem. Rev.* **1998**, *176*, 211. (b) Sheldrick, W. S.; Wachhold, M. *Angew. Chem., Int. Ed. Engl.* **1997**, *36*, 206. (c) Bowes, C. L.; Ozin, G. A. *Adv. Mater.* **1996**, *8*, 13. (d) Drake, G. W.; Kolis, J. W. *Coord. Chem. Rev.* **1994**, *137*, 131. (e) Kanatzidis, M. G.; Huang, S.-P. *Coord. Chem. Rev.* **1994**, *130*, 509. (f) Roof, L. C.; Kolis, J. W. *Chem. Rev.* **1993**, *93*, 1037. (g) Kanatzidis, M. G.; Das, B. K. *Comments Inorg. Chem.* **1999**, *21*, 29.
- (2) (a) Kanatzidis, M. G.; Sutorik, A. C. *Prog. Inorg. Chem.* **1995**, *43*, 151. (b) Kanatzidis, M. G. *Cur. Opin. Solid State Mater. Sci.* **1997**, *2*, 139. (c) Kanatzidis, M. G. *Phosphorus, Sulfur Silicon Relat. Elem.* **1994**, *93–94*, 159.
- (3) (a) Chou, J.-H.; Kanatzidis, M. G. *J. Solid State Chem.* **1996**, *123*, 115. (b) Chou, J.-H.; Hanko, J. A.; Kanatzidis, M. G. *Inorg. Chem.* **1997**, *36*, 4. (c) Chou, J.-H.; Kanatzidis, M. G. *Inorg. Chem.* **1994**, *33*, 1001. (d) Chou, J.-H.; Kanatzidis, M. G. *Chem. Mater.* **1995**, *7*, 5.
- (4) Wachhold, M.; Kanatzidis, M. G. *Inorg. Chem.* **1999**, *38*, 3863.

(5) Wachhold, M.; Kanatzidis, M. G. *Inorg. Chem.* **1999**, *38*, 4178.

(6) Kanatzidis, M. G.; Chou, J.-H. *J. Solid State Chem.* **1996**, *127*, 186.

containing strongly undulated chains ${}^1_{\infty}[\text{AsSe}_2]^-$ connected by distorted Ag^+ cations in trigonal planar and tetrahedral coordination, respectively. The Ag/AsSe_2 ratio is $1/4$ in **(I)** and $1/2$ in **(II)**, which leads to different sheet anions ${}^2_{\infty}[\text{AgAs}_4\text{Se}_8]^{3-}$ and ${}^2_{\infty}[\text{AgAs}_2\text{Se}_4]^-$, respectively. Both compounds represent *new* structure types.

Experimental Section

Reagents. Chemicals were used as obtained without further purification: Cs_2CO_3 , 99.9%, Aldrich Chemical Co.; CsCl , 99+%, Aldrich Chemical Co.; AgBF_4 , 99%, Strem Chemical; acetone, methanol, 99.9%, Mallinckrodt; diethyl ether, >99.0%, CCI. All experiments and manipulations were performed under an atmosphere of dry nitrogen inside a vacuum atmosphere Dri-Lab glovebox.

Synthesis. (a) Li_2Se . Li_2Se was prepared by reaction of stoichiometric amounts of lithium metal and black selenium in liquid ammonia.⁷

(b) Li_3AsSe_3 . Li_2Se and As_2Se_3 were ground thoroughly and mixed in a 1:3 ratio to load into a quartz tube (outer diameter 13 mm, wall thickness 0.8 mm). The tube was sealed under vacuum ($\sim 10^{-4}$ mbar) and then heated to 300 °C in 10 h and subsequently to 450 °C in 96 h and isothermed at this temperature for 100 h. After the sample was cooled to room temperature (100 h), dark-brown Li_3AsSe_3 was isolated and ground to a powder. Semiquantitative microprobe analysis (energy dispersive spectrometry; EDS) confirmed the As/Se ratio of 1:3, and the X-ray diffraction pattern indicated that this phase is not isostructural to the corresponding Na^+ or K^+ phases,⁸ which possess, among others,⁹ the Na_3AsS_3 structure type.¹⁰

(c) $\text{Cs}_3\text{AgAs}_4\text{Se}_8$. The compound was synthesized by the reaction of 0.050 g (0.15 mmol) of Cs_2CO_3 , 0.030 g (0.15 mmol) of AgBF_4 , and 0.150 g (0.45 mmol) of Li_3AsSe_3 in 1 mL of MeOH. The starting materials were mixed thoroughly, loaded into a Pyrex tube (outer diameter 13 mm, wall thickness 1.6 mm, $\sim 10\text{ cm}^3$ volume), and sealed under vacuum. The initial pH was about 10. The tube was kept at 120 °C for 72 h. After the product was washed with water, acetone, and diethyl ether, orange needle-shaped crystals were obtained in $\sim 10\%$ yield, together with red chunky crystals of CsAsSe_2 ¹¹ as the major product (50%, based on Ag), and some large orange prisms that were not air stable and that turned out to be Cs_3AsSe_4 .¹² Semiquantitative analysis by an SEM/EDS technique on the orange crystals gave $\text{Cs}_{3.16}\text{Ag}_{1.00}\text{As}_{5.81}\text{Se}_{11.97}$. The X-ray diffraction pattern of collected and ground orange crystals showed that it was a pure phase.

(d) $\text{CsAgAs}_2\text{Se}_4$. The compound was synthesized by the reaction of 0.035 g (0.2 mmol) of CsCl , 0.020 g (0.1 mmol) of AgBF_4 , and 0.105 g (0.3 mmol) of Li_3AsSe_3 in 1 mL of MeOH (initial pH ~ 8). The starting materials were sealed under vacuum in a Pyrex tube and kept at 140 °C for 70 h. Small, red, almost pure rhombic crystals were obtained ($\sim 70\%$ yield), together with some black amorphous powder. The compound was washed with water, acetone, and ether. Semiquantitative microprobe analysis on single crystals gave the stoichiometry as $\text{Cs}_{1.05}\text{Ag}_{1.00}\text{As}_{2.08}\text{Se}_{3.93}$. The powder X-ray diffraction pattern of the homogenized and ground material indicated a pure phase.

Physicochemical Methods. (a) Solid-State UV/Vis Spectroscopy. The single-crystal UV/vis spectrum of **I** was recorded at room temperature on a computer-controlled Hitachi FT spectrometer U6000 associated with an Olympus BH2-UMA microscope in the wavelength range 380–900 nm. UV–vis–near-IR diffuse reflectance spectra of a bulk powder sample of **II** was obtained on a Shimadzu UV-3101PC

Table 1. Crystal Data and Structure Refinement for $\text{Cs}_3\text{AgAs}_4\text{Se}_8$ (**I**) and $\text{CsAgAs}_2\text{Se}_4$ (**II**)

	I	II
empirical formula	$\text{Cs}_3\text{AgAs}_4\text{Se}_8$	$\text{CsAgAs}_2\text{Se}_4$
cryst color and habit	orange needle	red plate
fw [g mol ⁻¹]	1437.96	706.46
temp [K]	298	298
cryst syst	monoclinic	monoclinic
space group	$C2/c$ (No. 15)	$P2_1/c$ (No. 14)
<i>a</i> [Å]	25.212(2)	10.9211(1)
<i>b</i> [Å]	8.0748(7)	6.5188(2)
<i>c</i> [Å]	22.803(2)	13.7553(3)
β [deg]	116.272(1)	108.956(1)
<i>V</i> [Å ³]	4162.8(6)	926.17(4)
<i>Z</i>	8	4
ρ_{calc} [g cm ⁻³]	4.589	5.067
μ (Mo K α) [mm ⁻¹]	26.417	28.772
final <i>R</i> indices ^a [<i>I</i> > 2 σ (<i>I</i>)]	$R_1 = 0.0758$, w $R_2 = 0.1101$	$R_1 = 0.0578$, w $R_2 = 0.1164$

$$^a R_1 = \sum ||F_o| - |F_c|| / \sum |F_o|; wR_2 = [\sum w\{|F_o| - |F_c|\}^2 / \sum w|F_o|^2]^{1/2}, w = 1/\sigma^2\{|F_o|\}.$$

double-beam, double-monochromator spectrophotometer in the wavelength range 200–2500 nm. BaSO_4 powder was used as a reference (100% reflectance) and base material on which the ground powder sample was coated. Diffuse reflectance data were converted to absorbance data as described elsewhere.¹³ The band gap energy values were determined by extrapolation from the linear portion of the absorption edge in a (α /S) versus energy (eV) plot.

(b) Differential Thermal Analysis (DTA). DTA experiments were performed on a computer-controlled Shimadzu DTA-50 thermal analyzer. Typically, 10–20 mg of ground material was sealed in a carbon-coated quartz ampule under vacuum. A sealed quartz ampule of equal mass filled with Al_2O_3 was used as a reference. The sample was heated to the desired temperature at 5 °C/min and isothermed for 1 min followed by cooling at -5 °C/min to 50 °C. The sample stability was monitored by running a second heating/cooling cycle. The residues were examined by X-ray powder diffraction.

(c) Raman Spectroscopy. Raman spectra of suitable crystals with a clean surface were recorded on a Holoprobe Raman spectrograph equipped with a 633 nm helium–neon laser and a CCD camera detector. The instrument was coupled to an Olympus BX60 microscope. The spot size of the laser beam was 10 mm when a 50 \times objective lens was used.

(d) Semiquantitative Microprobe Analysis. The analyses were performed using a JEOL JSM-35C scanning electron microscope (SEM) equipped with a Tracor Northern EDS detector. Data were acquired on several crystals using an accelerating voltage of 20 kV and 45 s accumulation time.

(e) X-ray Crystallography. Single crystals of orange **I** and red **II** (crystal sizes: **I**, 0.20 mm \times 0.05 mm \times 0.05 mm; **II**, 0.22 mm \times 0.12 mm \times 0.05 mm) were sealed in glass capillaries (outer diameter 0.5 mm, wall thickness $1/100$ mm) and mounted on a goniometer head. Crystallographic data sets for **I** and **II** were collected on a Siemens Platform CCD diffractometer using graphite monochromatized Mo K α radiation (Table 1). The initial unit cells were refined with at least 200 reflections extracted from either matrix data or frames of the full data collection. Data were collected over a full sphere of reciprocal space, up to 61° and 57.6° in 2θ for **I** and **II**, respectively. The individual frames were measured with an ω rotation of 0.3° and acquisition times of 45 (**I**) and 30 (**II**) s. The SMART¹⁴ software was used for the data acquisition and SAINT¹⁵ for the data extraction and reduction, during which the unit cells were refined consecutively after every 100 frames. The absorption correction was performed using SADABS.¹⁶ Structure

(7) Fehér, F. In *Handbuch der präparativen Anorganischen Chemie*; Brauer, G., Ed.; Ferdinand Enke Verlag: Stuttgart, Germany, 1975; Band 1, p 372f.

(8) Bronger, W.; Donike, A.; Schmitz, D. Z. *Anorg. Allg. Chem.* **1998**, 624, 553.

(9) (a) Bronger, W.; Donike, A.; Schmitz, D. Z. *Anorg. Allg. Chem.* **1996**, 622, 1003. (b) Lin, J.; Miller, G. J. *J. Solid State Chem.* **1994**, 113, 296.

(10) (a) Hoppe, R.; Sommer, H. Z. *Anorg. Allg. Chem.* **1977**, 430, 199. (b) Palazzi, M. *Acta Crystallogr. B* **1976**, 32, 2175.

(11) Sheldrick, W. S.; Häusler, H. J. Z. *Anorg. Allg. Chem.* **1988**, 561, 139.

(12) Wachhold, M.; Sheldrick, W. S. Z. *Naturforsch.* **1996**, B51, 36.

(13) Zhang, X.; Kanatzidis, M. G. *J. Am. Chem. Soc.* **1994**, 116, 1890.

(14) SMART, version 5; Siemens Analytical X-ray Systems, Inc.: Madison, WI, 1998.

(15) SAINT, version 4; Siemens Analytical X-ray Systems, Inc.: Madison, WI, 1994–1996.

(16) Sheldrick, G. M. SADABS; University of Göttingen: Göttingen, Germany.

Table 2. Atomic Coordinates and Equivalent Isotropic Displacement Parameters [\AA^2] for Cs₃AgAs₄Se₈ (**I**) and CsAgAs₂Se₄ (**II**)^a

	<i>x</i>	<i>y</i>	<i>z</i>	<i>U</i> _{eq}	sof
I					
Cs1	0.25	0.25	0.5	0.038(1)	1
Cs2	0.1952(1)	0.6425(2)	0.2330(1)	0.040(1)	1
Cs3	0.4284(1)	0.1882(2)	0.4970(1)	0.049(1)	1
Cs4	0.0	-0.2622(2)	0.25	0.051(1)	1
Ag	0.2431(1)	0.6493(2)	0.4115(1)	0.038(1)	1
As1	0.1352(1)	0.1688(2)	0.1179(1)	0.028(1)	1
As2	0.1535(1)	-0.0200(2)	0.3198(1)	0.030(1)	1
As3	0.1548(1)	-0.2006(2)	0.4673(1)	0.026(1)	1
As4	0.0459(1)	0.2489(2)	0.1989(1)	0.036(1)	1
Se1	0.0556(1)	0.0311(2)	0.1299(1)	0.039(1)	1
Se2	0.3066(1)	0.4410(2)	0.3818(1)	0.032(1)	1
Se3	0.0770(1)	0.2180(3)	0.0014(1)	0.043(1)	1
Se4	0.1389(1)	0.5717(2)	0.3986(1)	0.032(1)	1
Se5	0.1083(1)	0.0296(2)	0.3929(1)	0.033(1)	1
Se6	0.2560(1)	-0.0398(2)	0.3827(1)	0.036(1)	1
Se7	0.1481(1)	0.2589(2)	0.2829(1)	0.041(1)	1
Se8	0.0458(1)	0.4904(2)	0.1446(1)	0.044(1)	1
II					
Cs	0.6192(1)	0.0014(2)	0.8193(1)	0.020(1)	1
Ag	0.5086(1)	-0.2333(2)	0.5094(1)	0.026(1)	1
As1	0.2851(2)	0.0952(3)	0.6233(2)	0.010(1)	0.827(4)
As2	0.3706(2)	-0.3859(3)	0.6988(2)	0.010(1)	0.827(4)
Se1	0.7171(1)	0.0131(3)	0.5397(1)	0.017(1)	1
Se2	0.4118(2)	0.4446(5)	0.8628(2)	0.012(1)	0.827(4)
Se3	0.9514(1)	-0.0178(3)	0.8400(1)	0.019(1)	1
Se4	0.6853(2)	0.0684(4)	0.0911(2)	0.013(1)	0.827(4)
AsA	0.2865(9)	0.901(2)	0.6238(8)	0.020(3)	0.173(4)
AsB	0.369(2)	0.382(2)	0.6988(9)	0.023(3)	0.173(4)
SeA	0.686(2)	0.935(2)	0.0901(8)	0.022(3)	0.173(4)
SeB	0.413(2)	0.551(2)	0.862(2)	0.021(3)	0.173(4)

^a The equivalent displacement factor is defined as one-third of the trace of the orthogonalized U^{ij} tensor.

solutions and refinements were performed with the SHELXTL package of crystallographic programs.¹⁷ Both structures were solved by direct methods in monoclinic space groups, i.e., $C2/c$ for Cs₃AgAs₄Se₈ (**I**) and $P2_1/n$ for CsAgAs₂Se₄ (**II**) (see Table 1). After the anisotropic refinement of all atom positions in **I**, the remaining electron density peak/hole was 2.277/-1.713 e/ \AA^3 , with all peaks being very close to heavy atom positions (<1.3 \AA). The final R values were $R_1 = 7.58$ and $wR_2 = 11.01\%$. The structure solution of **II** also gave immediately the heavy atom positions, but after the following anisotropic refinement of these atoms it was obvious that there were still four high peaks remaining in the electron density map. Furthermore, the refinement parameters were still quite high with $R_1 = 11.47\%$ and $wR_2 = 24.13\%$. The peaks were too close to the already refined atoms As1-Se2-As2-Se4, which define the central atoms of the $[\text{AsSe}_2]^-$ chain (see Table 2 and Figure 5), but they seemed to define a second $[\text{AsSe}_2]^-$ chain. Additionally, the terminal atoms Se1 and Se3 of the first chain, which coordinate to the Ag atoms, seemed to have reasonable values for typical As-Se₁ distances for two of the four peaks. A careful analysis of all distances and angles led to the conclusion that these new positions define the atom positions of a second (-As-Se)- chain (sequence AsA-SeA-AsB-SeB), which is disordered with the former one. Hereby the terminal Se atoms Se1 and Se3 of the first chain also serve as the third bonding partner for AsA and AsB in the second chain. The occupation factors of each set of four atoms of both chains were coupled and refined. Rather than leading to an expected 50%:50% ratio, we observed occupation probabilities of 82.7(4)% and 17.3(4)% for chains 1 and 2, respectively, with final refinement parameters of $R_1 = 5.78\%$ and $wR_2 = 11.64\%$. To figure out if this ratio is "accidental" (e.g., a product of the present crystallization conditions), we performed the refinement of a second crystal from a new reaction batch, giving a very similar ratio of 86.5(5)% to 13.5(5)%. To exclude the origin of

Table 3. Bond Lengths [\AA] and Angles [deg] for Cs₃AgAs₄Se₈ (**I**) and CsAgAs₂Se₄ (**II**)

Bond Lengths for I			
Ag-Se4	2.587(2)	As2-Se3	2.412(2)
Ag-Se2	2.611(2)	As2-Se5	2.439(2)
Ag-Se6	2.651(2)	As3-Se6	2.341(3)
Ag-As2	2.853(2)	As3-Se7	2.387(2)
As1-Se2	2.352(2)	As3-Se5	2.433(2)
As1-Se1	2.413(2)	As4-Se8	2.311(2)
As1-Se3	2.434(3)	As4-Se7	2.438(3)
As2-Se4	2.332(2)	As4-Se1	2.443(3)
Selected Bond Angles for I			
Se4-Ag-Se2	121.57(8)	Se4-As2-Se3	104.35(9)
Se4-Ag-Se6	115.55(8)	Se4-As2-Se5	104.28(9)
Se3-Ag-Se2	112.89(7)	Se3-As2-Se5	93.42(9)
Se2-Ag-As2	87.15(7)	Se6-As3-Se7	98.97(9)
Se4-Ag-As2	125.49(7)	Se6-As3-Se5	108.40(9)
Se6-Ag-As2	86.83(6)	Se7-As3-Se5	96.61(9)
Se1-As1-Se2	100.86(9)	Se8-As4-Se7	98.22(10)
Se2-As1-Se3	101.77(9)	Se8-As4-Se1	103.81(9)
Se1-As1-Se3	93.97(9)	Se7-As4-Se1	99.11(9)
Bond Lengths for II			
Ag-Se1	2.706(2)	As2-Se4	2.400(3)
Ag-Se3	2.709(2)	As2-Se2	2.420(3)
Ag-Se3A	2.739(2)	AsA-Se1	2.304(11)
Ag-Se1A	2.740(2)	AsA-SeA	2.429(16)
Ag-AsA	3.053(3)	AsA-SeB	2.455(16)
As1-Se1	2.343(2)	AsB-Se3	2.286(10)
As1-Se4	2.425(3)	AsB-SeA	2.393(16)
As1-Se2	2.427(3)	AsB-SeB	2.429(16)
As2-Se3	2.340(2)		
Selected Bond Angles for II			
Se1-Ag-Se3	119.66(5)	Se1-AsA-SeA	99.8(5)
Se1-Ag-Se3A	112.33(6)	Se1-AsA-SeB	104.3(5)
Se3-Ag-Se3A	109.00(6)	SeA-AsA-SeB	90.8(5)
Se1-Ag-Se1A	106.61(6)	Se3-AsB-SeA	108.7(5)
Se3-Ag-Se1A	97.82(5)	Se3-AsB-SeB	99.3(5)
Se3A-Ag-Se1A	110.22(4)	SeA-AsB-SeB	103.2(6)
Se1-As1-Se4	103.5(1)	As1-Se2-As2	89.3(1)
Se1-As1-Se2	102.7(1)	As1-Se4-As2	95.55(9)
Se2-As1-Se4	91.33(10)	AsA-SeA-AsB	95.4(5)
Se3-As2-Se4	105.88(10)	AsA-SeB-AsB	88.8(6)
Se2-As2-Se3	97.36(9)	Ag-Se1-AgA	68.18(6)
Se2-As2-Se4	102.32(11)	Ag-Se3-AgA	79.61(6)

this ratio in a possible supercell setting in some direction of the unit cell, we made additional investigations; zone photos on the CCD diffractometer with long exposure times (>10 min) gave no evidence for the presence of supercell reflections at room temperature or at -120 °C. Also, transmission electron microscopic (TEM) investigations were unsuccessful in finding such a supercell.

Complete data collection parameters and details of the structure solution and refinement for **I** and **II** are given in Table 1. Fractional atomic coordinates, equivalent isotropic displacement parameters (U_{eq}), and occupation factors are given in Table 2, and bond distances and angles are given in Table 3.

Results and Discussion

Synthesis. The reaction of AgBF_4 with Li_3AsSe_3 in MeOH in the presence of an alkali metal source for Cs^+ provides two new quaternary silver selenoarsenates with novel anionic layer structure types, depending on conditions and reactants.

The use of Cs_2CO_3 as a "basic cation" source leads to $\text{Cs}_3\text{AgAs}_4\text{Se}_8$ (**I**) as an accessible quaternary product, together with the known phase CsAsSe_2 .¹¹ If CsCl is used instead, we obtain $\text{CsAgAs}_2\text{Se}_4$ (**II**) under otherwise very similar conditions. Presumably, **I** forms under more basic conditions because Cs_2CO_3 gives rise to higher pH solutions than CsCl . This clearly demonstrates the importance of the reaction conditions for different possible reaction paths. So far, *time-*

(17) Sheldrick, G. M. *SHELXTL*, version 5.1; Siemens Analytical X-ray Systems, Inc.: Madison, WI, 1997.

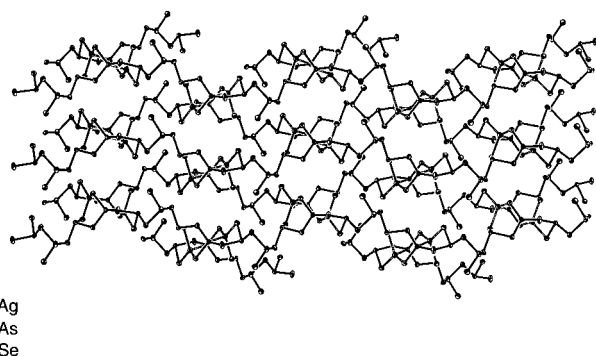


Figure 1. ${}^2_{\infty}[\text{AgAs}_4\text{Se}_8]^{3-}$ layer of $\text{Cs}_3\text{AgAs}_4\text{Se}_8$ (**I**) viewed approximately from the $[10\ 0\ 1]$ direction. The layers contain large cavities able to capture three of the four crystallographically different Cs^+ cations (50% probability thermal vibrational ellipsoids).

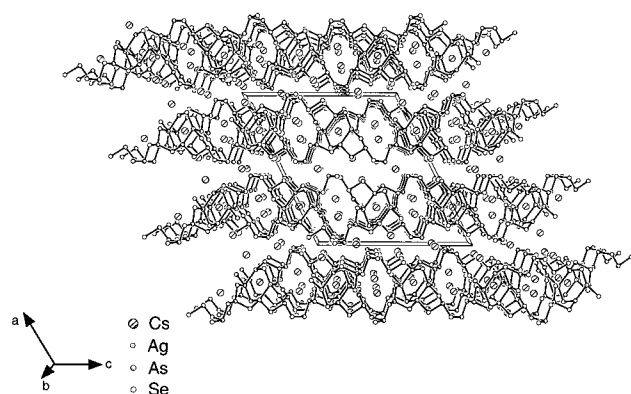


Figure 2. Unit cell of **I** viewed from the $[010]$ direction. The thickness of one ${}^1_{\infty}[\text{AgAs}_4\text{Se}_8]^{3-}$ layer anion is about 11.3 Å, the layers are separated by the Cs atoms.

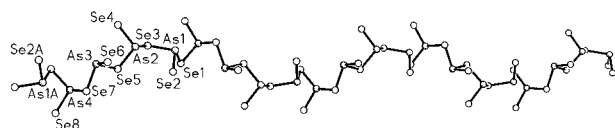


Figure 3. "Achter" single chain ${}^1_{\infty}[\text{AsSe}_2]^{-}$ of **I** viewed from $[100]$ direction. Identity is reached after every eight AsSe_3 units. The repeating length is 22.803 Å, identical to the b direction of the unit cell.

dependent products could not be observed in this reaction system, as it was possible for the alkali metals K and Rb.^{4,5} Short reaction times only led to known ternary compounds or amorphous products.

Structure of $\text{Cs}_3\text{AgAs}_4\text{Se}_8$ (I**).** The anion structure of $\text{Cs}_3\text{AgAs}_4\text{Se}_8$ (**I**) consists of parallel ${}^2_{\infty}[\text{AgAs}_4\text{Se}_8]^{3-}$ double layers (Figure 1), which lie within the bc plane of the monoclinic cell (Figure 2). The double layers possess an *open structure* with large holes capable of accommodating three of the four crystallographically distinguishable Cs^+ cations (Figures 1 and 2). The fourth Cs^+ cation lies between the neighboring ${}^2_{\infty}[\text{AgAs}_4\text{Se}_8]^{3-}$ sheets and separates them from each other (Figure 2).

The layers are built of undulating ${}^1_{\infty}[\text{AsSe}_2]^{-}$ chains (Figure 3) running down the c direction of the unit cell (Figure 1). Since identity within the chain is reached after a sequence of eight AsSe_3 units, they can be classified as a "achter" single chain (Figure 3), according to the nomenclature proposed by Liebau.¹⁸ This is the highest value so far observed for a chalcogenidoarsenate chain. The As–Se bond lengths of the terminal Se

Table 4. Torsion Angles of the $[\text{AsSe}_2]^{-}$ Chains in $\text{Cs}_3\text{AgAs}_4\text{Se}_8$ (**I**) and $\text{CsAgAs}_2\text{Se}_4$ (**II**)^a

I		II	
Se1–As1–Se3–As2	−147.9(1)	<i>chain 1</i>	
As1–Se3–As2–Se5	+120.3(1)	As1–Se2–As2–Se4	+69.7(1)
Se3–As2–Se5–As3	−155.0(1)	Se2–As2–Se4–As1	−56.2(1)
As2–Se5–As3–Se7	+153.9(1)	As2–Se4–As1–Se2	+138.1(1)
Se5–As3–Se7–As4	−82.8(1)	Se4–As1–Se2–As2	−72.2(1)
As3–Se7–As4–Se1	+60.8(1)	<i>chain 2</i>	
Se7–As4–Se1–As1	−54.0(1)	AsA–SeA–AsB–SeB	+55.2(1)
As4–Se1–As1–Se3	+113.6(1)	SeA–AsB–SeB–AsA	−70.0(1)
		AsB–SeB–AsA–SeA	+72.9(1)
		SeB–AsA–SeA–AsB	−137.4(1)

^a Identity within the chain is reached after every eighth and fourth As atom. Therefore they can be classified as "achter" and "vierer" single chains, respectively.¹⁸ The torsion angle sequence of the two disordered chains in **II** are very similar.

(As–Se_t, 2.311(2)–2.352(2) Å) atoms are, as expected, shorter than the ones of the bridging Se atom (As–Se_b, 2.387(2)–2.443(2) Å). All As–Se_b–As, Se_t–As–Se_b, and Se_t–As–Se_t angles are within the expected ranges (93.42(9)°–108.40(9)°) and agree well with the ones found in other ${}^1_{\infty}[\text{AsSe}_2]^{-}$ chains^{11,19} (see Table 3). The undulation of the chain is also mirrored in its torsion angles, which range from 54.0(1)° to 155.0(1)° (Table 4).

The ${}^1_{\infty}[\text{AsSe}_2]^{-}$ chains of two neighboring layers are now connected by Ag^+ atoms to form the 2D sheet anion ${}^2_{\infty}[\text{AgAs}_4\text{Se}_8]^{3-}$. Two of those "double layers" fit within the a direction of the unit cell (Figure 2), and a single layer has a thickness of approximately 11.3 Å. Every Ag^+ is coordinated to only two ${}^1_{\infty}[\text{AsSe}_2]^{-}$ chains, and as the formula implies, there is only one coordinating Ag^+ per four AsSe_3 units. The coordination sphere of the Ag^+ atom consists of three Ag–Se bonds (2.611(2)–2.651(2) Å) completed by a longer $\text{Ag}\cdots\text{As}$ contact of 2.853(2) Å. The latter is responsible for a small distortion of the trigonal planar AgSe_3 coordination mode (see angles at the Ag^+ ion; Table 3). The distances of the atoms in the AgSe_3 fragment from its least-squares plane are as follows, Se2 +0.1215 Å, Se4 +0.1265 Å, Se6 +0.1121 Å, Ag −0.3601, whereas for As2 it is −2.9571 Å. There are no significant $\text{Ag}\cdots\text{Ag}$ contacts, with the shortest occurring at 4.220(3) Å (Figure 4). The structure of **I** can also be described as large $[\text{Ag}_2\text{As}_6\text{Se}_{14}]^{8-}$ clusters (Figure 4) that condense through common AsSe_3 units (i.e., As4; see Figures 1 and 4) to form the sheet anion ${}^2_{\infty}[\text{AgAs}_4\text{Se}_8]^{3-}$. The *volume* and *shape* of the cluster are therefore responsible for the fact that an open structure with large holes is obtained incorporating the alkali metal cations (compare Figures 4 and 1). The coordination polyhedra of the four Cs^+ ions are irregular with coordination numbers between 8 and 11 and Cs–Se distances in the range 3.545(3)–4.298(3) Å.

Structure of $\text{CsAgAs}_2\text{Se}_4$ (II**).** $\text{CsAgAs}_2\text{Se}_4$ (**II**) forms another layered structure type that is not known in other alkali metal–Ag–As–Se systems.^{4–6} Its structure is assembled from strongly undulated polar ${}^1_{\infty}[\text{AsSe}_2]^{-}$ chains that are connected by Ag^+ atoms to form a ${}^2_{\infty}[\text{AgAs}_2\text{Se}_4]^{-}$ sheet anion (Figure 5). The strong undulation becomes apparent through the torsion angles of the central atoms of the ${}^1_{\infty}[\text{AsSe}_2]^{-}$ chain, with three of the four different angles having very small values ranging from 56.2(1)° to 72.2(1)° (see Table 4). The ${}^2_{\infty}[\text{AgAs}_2\text{Se}_4]^{-}$ layers lie within the (101) planes of the unit cell and are separated by the Cs^+ cations (Figure 6). All bond parameters are very similar to the ones found in **I**; this time the Ag^+ ion is

(18) Liebau, F. *Naturwissenschaften* **1962**, 49, 41.

(19) Eisenmann, B.; Schäfer, H. Z. *Anorg. Allg. Chem.* **1979**, 456, 87.

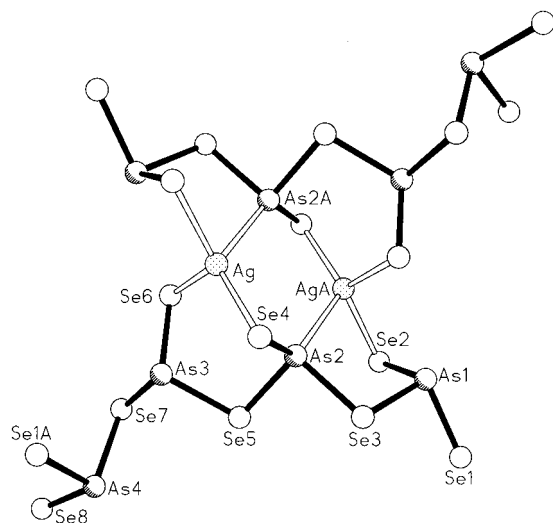


Figure 4. Alternative description of the structure of **I** leads to the identification of large $[\text{Ag}_2\text{As}_6\text{Se}_{14}]^{8-}$ clusters, which condense through $[\text{AsSe}_3]^{3-}$ units (As4) to form the $^{2-}[\text{AgAs}_4\text{Se}_8]^{3-}$ sheet anion in Figure 1. The nonbonding $\text{Ag}\cdots\text{Ag}$ contacts is 4.220(3) Å.

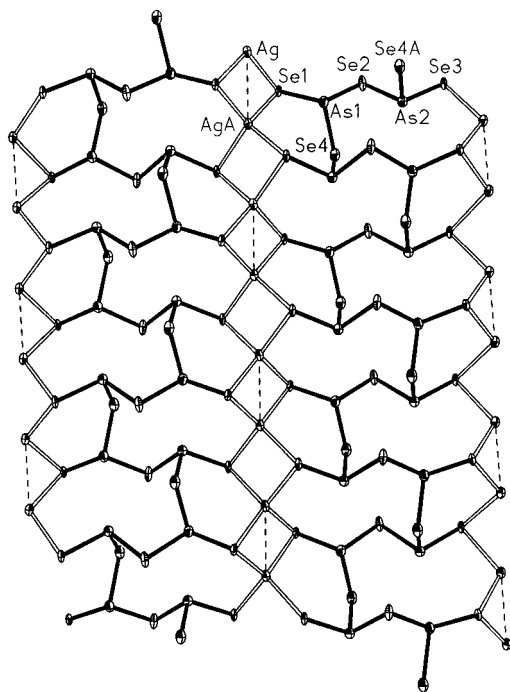


Figure 5. (a) Sheet anion $^{2-}[\text{AgAs}_2\text{Se}_4]^{-}$ of $\text{CsAgAs}_2\text{Se}_4$ (**II**), consisting of undulated $^{1-}[\text{AsSe}_2]^{-}$ chains, which are connected by tetrahedral Ag^+ cations (50% probability thermal vibrational ellipsoids). The Ag^+ ions lie in a row with alternating short and long distances of 3.053(3) Å (dotted lines) and 3.488(3) Å (nonbonding).

coordinated in a very regular tetrahedral manner by four Se_i atoms of the chains, with $\text{Ag}-\text{Se}$ bond lengths between 2.706 and 2.740(2) Å (Table 3). The Ag^+ cations lie between the $^{1-}[\text{AsSe}_2]^{-}$ chains, with alternating short and long $\text{Ag}\cdots\text{Ag}$ distances of 3.053(3) and 3.488(3) Å as interacting and noninteracting distances, respectively (Figure 5). Therefore, a very interesting and unique “ $^{1-}[\text{Ag}_2]^{2+}$ ” chain results, with all $[\text{Ag}_2]^{2+}$ dumbbells lined up in a row. We also observed such characteristic Ag^+ dumbbell units in previous studies of selenoarsenate compounds, e.g., $\text{K}_3\text{AgAs}_2\text{Se}_5 \cdot 0.25\text{MeOH}$, $\text{K}_2\text{AgAs}_3\text{Se}_6$, $\text{Rb}_2\text{AgAs}_3\text{Se}_6$,⁴ and $\text{RbAg}_2\text{As}_3\text{Se}_6$.⁵ Compounds showing interactions between cations with closed d^{10} configura-

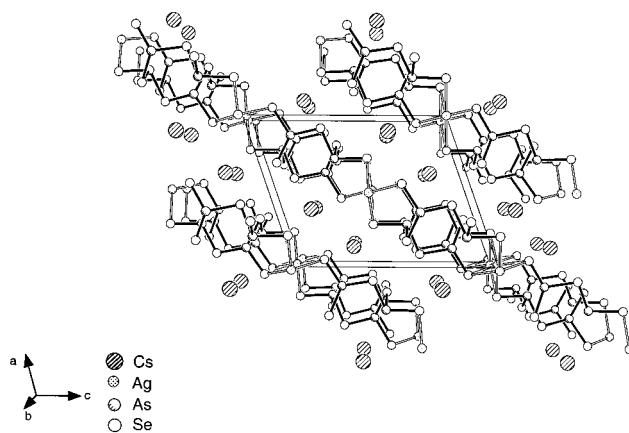


Figure 6. Unit cell of **II** viewed from the [010] direction. The $^{2-}[\text{AgAs}_2\text{Se}_4]^{-}$ layers lie within the (101) planes.

tions have been of special interest in recent years, since this feature can influence their physical and chemical properties (e.g., the color or electrical conductivity).²⁰

The most interesting feature of this compound is the “perfect disorder” of the $^{1-}[\text{AsSe}_2]^{-}$ chains, becoming possible by the special way of chain undulation. The *polar* chains run down the *b* direction of the unit cell (Figure 5, 7a) and identity is reached at every fourth As atom; therefore, they can be classified as “vierer” single chains.¹⁸ The mirror plane at $b = 0.25$ (space group $P2_1/n$) leads to a symmetry-related chain (Figure 7b) with atom positions $(x; 1 - y; z)$ that overlay the first one (compare Figures 7a-c) and with polarity that heads in the opposite direction. Only the central $(-\text{As}-\text{Se})-$ chain atoms (chain 1, As1–Se2–As2–Se4) are affected by the mirror plane and transform in to a new chain 2 (sequence AsA–SeA–AsB–SeB), changing therefore the polarity direction. Since the *y* coordinates of the Se_i atoms in the $^{1-}[\text{AsSe}_2]^{-}$ chains (Se1, Se3) are very close to zero (see Table 2), their positions are not affected. As a result, Se1 and Se3 still serve perfectly as terminal bonding partners for the disordered As1/AsA and As3/AsB atom pairs (Table 3, Figure 7c). Both chains have very similar conformations, which becomes evident through their almost identical torsion angles (see Table 4). The occupancy of chains 1 and 2 are 82.7(4)% and 17.3(4)%, respectively, because both X-ray zone photos and transmission electron microscopic investigations gave no hints for the presence of a supercell. Therefore, we assume we are dealing with a crystallization twin.

The only crystallographic Cs⁺ cation is 8-fold-coordinated by six Se and two As atoms (3.548(2)–3.937(1) Å) and forms an irregular coordination polyhedron.

Properties. The thermal behavior of $\text{Cs}_3\text{AgAs}_4\text{Se}_8$ (**I**) and $\text{CsAgAs}_2\text{Se}_4$ (**II**) was investigated by differential thermal analysis (DTA) in the range 25–400 °C. Both **I** and **II** melt incongruently at about 265 and 281 °C, respectively. They do not show any transitions upon cooling, which is consistent with an incongruent melting point. A second heating/cooling cycle showed no transitions up to 400 °C. The X-ray powder patterns of the residues show that in both cases elemental Se is present. No further peaks could be identified, leading to the assumption that other products were amorphous. This is in agreement with the proposal that **I** and **II** are kinetically stabilized products that decompose at higher temperatures and are therefore probably not accessible via classical high-temperature direct combination

(20) (a) Jansen, M. *Angew. Chem., Int. Ed. Engl.* **1987**, 26, 1098. (b) Pyykko, P. *Chem. Rev.* **1997**, 97, 597.

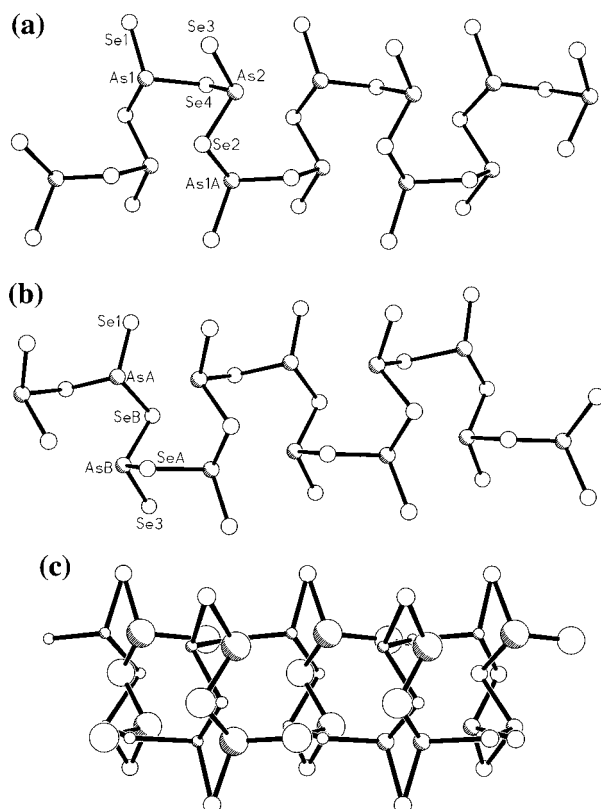


Figure 7. “Perfectly disordered” ${}^1\infty[\text{AsSe}_2]^-$ chains in **II**, which run down the *b* axis of the unit cell: (a) chain 1, (b) chain 2, (c) overlay of both chains. The occupancies of chains 1 and 2 are 82.7% and 17.3–(4)%, which is taken into account in the figure by using huge and small balls for the atoms in (c). This figure also reveals that the disorder only takes place within the central $-(\text{As}-\text{Se}_b-)$ chain (atom sequence $\text{As1}-\text{Se2}-\text{As2}-\text{Se4}$ for chain 1 and $\text{AsA}-\text{SeA}-\text{AsB}-\text{SeB}$ for chain 2). The terminal Se atoms (Se1 , Se3 , drawn as medium-sized balls), which coordinate the Ag^+ cations, do not change their positions and have perfect bond lengths for $\text{As1}/\text{AsA}$ and $\text{As2}/\text{AsB}$.

reactions, although they may be accessible through polychalcogenide fluxes.^{2a}

Optical transmission spectra (Figure 8) indicate that **I** and **II** are typical wide band gap semiconductors; the band gap of $\text{Cs}_3\text{AgAs}_4\text{Se}_8$ was found to be 2.07 eV, and the value for $\text{CsAgAs}_2\text{Se}_4$ is lower at 1.79 eV. Similar values have been obtained for other Ag selenoarsenates, e.g., $\text{K}_2\text{AgAs}_3\text{Se}_6$ or $\text{Rb}_2\text{AgAs}_3\text{Se}_6$.⁴

Raman spectra of well-grown single crystals were recorded between 75 and 2500 cm^{-1} for both compounds and are shown in Figure 9. The pattern is similar, showing a number of strong peaks between 200 and 300 cm^{-1} , with a maximum at 256 and 249 cm^{-1} for **I** and **II**, respectively. $\text{Cs}_3\text{AgAs}_4\text{Se}_8$ shows further peaks at 231(s), 244(m), 264(m), 277(m), and 285(m) cm^{-1} , and $\text{CsAgAs}_2\text{Se}_4$ shows peaks at 212(s), 235(s), 263(m), and 283(m) cm^{-1} (s = strong, m = medium). Both compounds also have several weaker modes between 75 and 150 cm^{-1} (Figure 9). Whereas the former region at higher frequencies is typical for As–Se and Ag–Se vibrations, the latter absorptions may be a result of collective lattice modes or vibrations associated with the Cs^+ cations. A comparison of **I** and **II** with the spectra of $\text{K}_2\text{AgAs}_3\text{Se}_6$ and $\text{Rb}_2\text{AgAs}_3\text{Se}_6$ ⁴ confirms the similarity in the pattern of ${}^1\infty[\text{AsSe}_2]^-$ chain containing compounds.

Concluding Remarks

The Cs–Ag–As–Se quaternary reaction system now contains the two new compounds $\text{Cs}_3\text{AgAs}_4\text{Se}_8$ (**I**) and $\text{CsAgAs}_2\text{Se}_4$

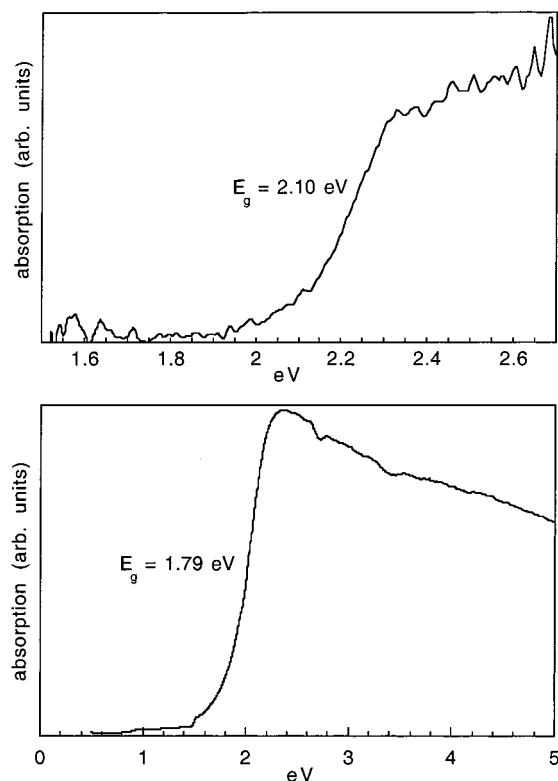


Figure 8. (a) Single-crystal UV–vis spectrum of $\text{Cs}_3\text{AgAs}_4\text{Se}_8$ (**I**). (b) UV–vis spectrum obtained from a polycrystalline powder sample of $\text{CsAgAs}_2\text{Se}_4$ (**II**).

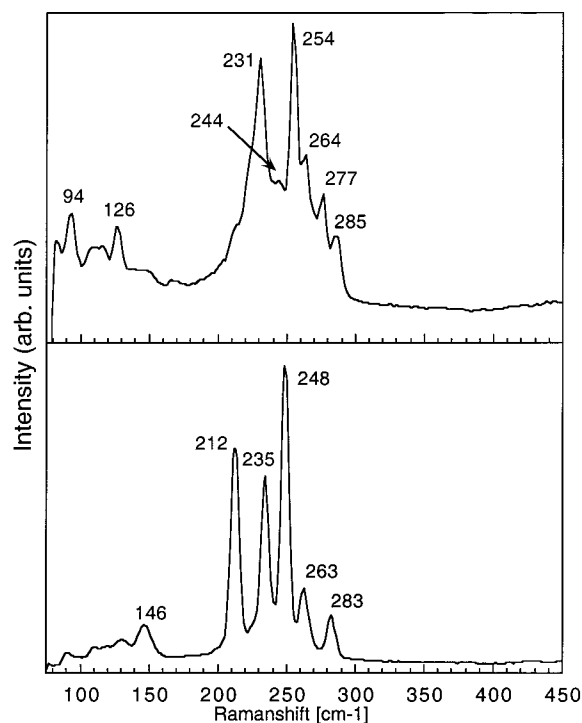


Figure 9. Raman spectra of single crystals of (a) $\text{Cs}_3\text{AgAs}_4\text{Se}_8$ (**I**) and (b) $\text{CsAgAs}_2\text{Se}_4$ (**II**).

Se_4 (**II**), which can be accessed with methanothermal reactions of AgBF_4 and Li_3AsSe_3 with Cs_2CO_3 and CsCl , respectively. Both compounds adopt new layered structure types not observed so far in other alkali metal–Ag–As–Se systems. As in the corresponding K or Rb systems,^{4,5} no time-dependent products could be found. In this case, pH-dependent products were

obtained, since the Cs₂CO₃ used in the synthesis for **I** provides a higher initial pH value than the CsCl used for **II**. Whereas the Ag⁺ ions in **I** show no close Ag···Ag interactions, contacts of 3.053(3) Å could be observed in **II**, leading to characteristic Ag₂²⁺ units, which have already been observed in a number of other silver selenoarsenates.^{4,5} The special conformation of the ¹_∞[AsSe₂][−] chain in **II** leads to a “perfect disorder” of the central (−As−Se)− chain with respect to the Ag⁺-coordinating terminal Se atoms, which remain unchained in position for both chains.

As a summary, the alkali metal−Ag−As−Se reaction system, with the heavier alkali metals K⁺, Rb⁺, and Cs⁺, has led to the synthesis of no less than *seven* quaternary compounds by solventothermal reactions, as well as the ternary product β-Ag₃−AsSe₃.^{4–6} Hereby the reaction products are strongly dependent on the reaction time and temperature as well as other parameters, such as the initial pH value or the reactants used. A higher degree of condensation of the initial [AsSe₃]^{3−} unit can generally be observed for longer reaction times.^{4,5} Short reaction times lead to [As₂Se₅]^{4−} Ψ-bitetrahedral units in K₃AgAs₂Se₅·0.25MeOH⁴ or [As₃Se₆]^{3−} rings in RbAg₂As₃Se₆.⁵ Prolonged reaction times of 70 h or more, on the other hand, lead to very

stable and flexible ¹_∞[AsSe₂][−] chains in K₂AgAs₃Se₆,⁴ Rb₂−AgAs₃Se₆,⁴ Cs₃AgAs₄Se₈ (**I**), and CsAgAs₂Se₄ (**II**). The conformations of the chains vary dramatically among structure types, and even more examples have been described in the literature.^{11,19}

Acknowledgment. Support from the National Science Foundation CHE 96-33798 (Chemistry Research Group) and the Petroleum Research Fund, administered by the American Chemical Society, is gratefully acknowledged. We acknowledge the use of the W. M. Keck Microfabrication Facility at Michigan State University, a NSF MRSEC facility. Part of this work was carried out at the facilities of the Center for Electron Optics of Michigan State University. M.W. thanks the Deutsche Forschungsgemeinschaft for a postdoctoral research fellowship.

Supporting Information Available: Tables of crystallographic data, fractional atomic coordinates, isotropic and anisotropic thermal parameters, and interatomic distances and angles for **I** and **II**. This material is available free of charge via the Internet at <http://pubs.acs.org>.

IC000027J